

Density Functional Theory Study of Nine-Atom Germanium Clusters: Effect of Electron Count on Cluster Geometry

R. B. King*[†] and I. Silaghi-Dumitrescu[‡]

Department of Chemistry, University of Georgia, Athens, Georgia 30602, and Faculty of Chemistry and Chemical Engineering, Babeş-Bolyai University, Cluj-Napoca, Roumania

Received March 20, 2003

Density functional theory (DFT) at the hybrid B3LYP level has been applied to the germanium clusters Ge_9^z clusters ($z = -6, -4, -3, -2, 0, +2, \text{ and } +4$) starting from three different initial configurations. Double- ζ quality LANL2DZ basis functions extended by adding one set of polarization (d) and one set of diffuse (p) functions were used. The global minimum for Ge_9^{2-} is the tricapped trigonal prism expected by Wade's rules for a $2n + 2$ skeletal electron structure. An elongated tricapped trigonal prism is the global minimum for Ge_9^{4-} similar to the experimentally found structure for the isoelectronic Bi_9^{5+} . However, the capped square antiprism predicted by Wade's rules for a $2n + 4$ skeletal electron structure is only 0.21 kcal/mol above this global minimum indicating that these two nine-vertex polyhedra have very similar energies in this system. Tricapped trigonal prismatic structures are found for both singlet and triplet Ge_9^{6-} , with the latter being lower in energy by 3.66 kcal/mol and far less distorted. The global minimum for the hypoelectronic Ge_9 is a bicapped pentagonal bipyramid. However, a second structure for Ge_9 only 4.54 kcal/mol above this global minimum is the C_{2v} flattened tricapped trigonal prism structure found experimentally for the isoelectronic Tl_9^{9-} . For the even more hypoelectronic Ge_9^{2+} , the lowest energy structure consists of an octahedron fused to two trigonal bipyramids. For Ge_9^{4+} , the global minimum is an oblate (squashed) pentagonal bipyramid with two pendant Ge vertices.

1. Introduction

Previous papers from our group discuss our results from density functional theory (DFT) computations on six-vertex atom clusters of the group 13 elements boron, indium, and thallium^{1,2} and on five-, six-, and seven-atom clusters of germanium.³ A feature of these cluster sizes is the bipyramidal shape of the most spherical deltahedra,⁴ namely the trigonal bipyramid, octahedron, and pentagonal bipyramid for the five-, six-, and seven-vertex clusters, respectively. Our computations confirm the expectation from Wade's rules^{5,6} that the lowest energy structures for the n -vertex

clusters of these sizes with $2n + 2$ skeletal electrons are indeed these bipyramids. Furthermore, similar computations on hypoelectronic clusters of these sizes having fewer than $2n + 2$ skeletal electrons indicate interesting distortions from ideal bipyramidal symmetry.

We have now extended our DFT study to homoatomic clusters of more than seven atoms where the most spherical deltahedra⁴ are no longer bipyramids. The group 14 element germanium rather than the group 13 elements was chosen for this initial work in order to minimize the charges on clusters having the desired electron counts. Of particular interest are the nine-vertex Ge_9^z clusters since numerous nine-vertex homoatomic clusters of the group 13 and 14 elements with 20, 22, and 24 skeletal electrons are known experimentally⁷ in Zintl phases whereas similar eight-vertex clusters are rather rare. The properties of nine-vertex clusters (e.g., fluxionality as determined by NMR)^{8,9} suggest that two of the nine-vertex polyhedra, namely the tricapped trigonal

* To whom correspondence should be addressed. E-mail: rbking@sunchem.chem.uga.edu.

[†] University of Georgia.

[‡] Babeş-Bolyai University.

(1) King, R. B.; Silaghi-Dumitrescu, I.; Kun, A. *Inorg. Chem.* **2001**, *40*, 2450.

(2) King, R. B.; Silaghi-Dumitrescu, I.; Kun, A. In *Group 13 Chemistry: From Fundamentals to Applications*; Shapiro, P., Atwood, D. A., Eds.; American Chemical Society: Washington, DC, pp 208–225.

(3) King, R. B.; Silaghi-Dumitrescu, I.; Kun, A. *J. Chem. Soc., Dalton Trans.* **2002**, 3999.

(4) Williams, R. E. *Inorg. Chem.* **1971**, *10*, 210.

(5) Wade, K. *Chem. Commun.* **1971**, 792.

(6) Wade, K. *Adv. Inorg. Chem. Radiochem.* **1976**, *18*, 1.

(7) Fässler, T. F. *Coord. Chem. Rev.* **2001**, *215*, 347.

(8) Rudolph, R. W.; Wilson, W. L.; Parker, F.; Taylor, R. C.; Young, D. C. *J. Am. Chem. Soc.* **1978**, *100*, 4629.

(9) Rudolph, R. W.; Wilson, W. L.; Taylor, R. C. *J. Am. Chem. Soc.* **1981**, *103*, 2480.

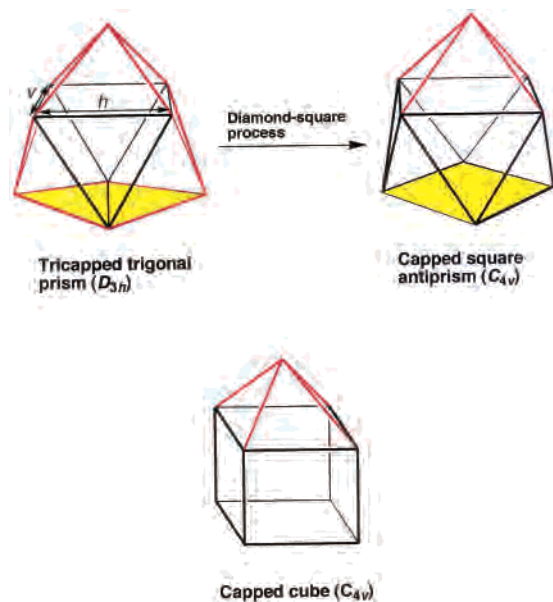


Figure 1. (a) Relationship between the tricapped trigonal prism and the capped square antiprism through a diamond-square process. The faces involved in the diamond-square process are indicated in yellow, and the edges to the caps are indicated in red. (b) Capped cube starting point used for some of the computations.

prism and the capped square antiprism, are of very similar energies in many systems.¹⁰ These two polyhedra are related by a simple diamond-square process involving rupture of a single edge with corresponding distortion of the vertex positions from D_{3h} to C_{4v} symmetry with a flat square face in the ideal capped square antiprism (Figure 1a). Furthermore, the nine-vertex most spherical deltahedron, namely the tricapped trigonal prism, is geometrically significant in being the smallest of the most spherical deltahedra in which the degree 5 vertices favored in boron clusters separate the degree 4 vertices leaving no edge joining two degree 4 vertices.¹¹

A number of calculations have been reported on nine-vertex germanium clusters with relatively low charges (0 and ± 1) in view of the relationships between the structures of the gas phase and bulk semiconducting germanium materials.^{12–16} However, reports of electronic structure calculations for Ge_9^z clusters with higher charges ($|z| > 1$) appearing in various Zintl phases are rather limited. Thus, extended Hückel molecular orbital studies on such clusters have been reported.^{17,18} However, to our knowledge only two recent papers^{19,20} use density functional methods for such systems.

- (10) Guggenberger, L. J.; Muetterties, E. L. *J. Am. Chem. Soc.* **1976**, *98*, 7221.
- (11) King, R. B. *Inorg. Chem.* **2001**, *40*, 6369.
- (12) Vasiliev, I.; Öğüt, S.; Chelikowsky, J. R. *Phys. Rev. Lett.* **1997**, *78*, 4805.
- (13) Öğüt, S.; Chelikowsky, J. R. *Phys. Rev. B* **1997**, *55*, R4914.
- (14) Li, B.-X.; Cao, P.-L. *Phys. Rev. B* **2000**, *62*, 15788.
- (15) Wang, J.; Wang, G.; Zhao, J. *Phys. Rev. B* **2001**, *64*, 205411.
- (16) Li, S.-D.; Zhao, Z.-G.; Wu, H.-S.; Jin, Z.-H. *J. Chem. Phys.* **2001**, *115*, 9255.
- (17) Belin, C.; Mercier, H.; Angilella, V. *New J. Chem.* **1991**, *15*, 951.
- (18) Lohr, L. L., Jr. *Inorg. Chem.* **1981**, *20*, 4229.
- (19) Hirsch, A.; Chen, Z.; Jiao, H. *Angew. Chem., Int. Ed.* **2001**, *40*, 2834.
- (20) Li, S.-D.; Guo, Q.-L.; Zhao, X.-F.; Wu, H.-S.; Jin, Z.-H. *J. Chem. Phys.* **2002**, *117*, 606.

Table 1. Optimized Structures for the Ge_9^z Clusters ($z = -6, -4, -3, -2, 0$, and $+2$)

cluster	final geometry	energy, ^a au	relative energy, kcal/mol	N_{imag}
Ge_9^{6-}	tricapped trigonal prism (triplet)	-33.015330 -34.500599	0	0
Ge_9^{6-}	distorted tricapped trigonal prism (singlet)	-33.009503 -34.476749	3.66 14.97	0
Ge_9^{4-}	tricapped trigonal prism	-33.742882 -34.475150	0	0
Ge_9^{4-}	capped square antiprism	-33.742553 -34.470183	0.21 3.10	1 (12i)
Ge_9^{4-}	capped bisdisphenoid	-33.704215 -34.331951	24.27 56.43	0
Ge_9^{3-}	tricapped trigonal prism	-33.998263 -34.422270	0	0
Ge_9^{2-}	tricapped trigonal prism	-34.168057 -34.359244	0	0
Ge_9^{2-}	capped bisdisphenoid	-34.141640 -34.331951	15.58 17.12	0
Ge_9^0	bicapped pentagonal bipyramid	-34.103370	0	0
Ge_9^0	Tl_9^{9-} structure (C_{2v})	-34.096130	4.54	0
Ge_9^{2+}	fusion of octahedron + 2 trigonal bipyramids	-33.455051	0	0
Ge_9^{2+}	fusion of octahedron + 2 tetrahedra	-33.446480	5.38	0
Ge_9^{4+}	pentagonal bipyramid + 2 pendant Ge atoms	-32.294498	0	0
Ge_9^{4+}	unsymmetrical open structure	-32.279412	9.47	0
Ge_9^{4+}	unsymmetrical open structure	-32.273674	13.07	0

^a For the negatively charged species, the second entries are the energies calculated when the effect of the counterions is simulated by a set of positive charges dispersed on the Connolly surface.

2. Computational Methods

Geometry optimizations were carried out at the hybrid DFT B3LYP level²¹ with the LANL2DZ double- ζ quality basis functions²² extended by adding one set of polarization (d) and one set of diffuse (p) functions.²³ The Gaussian 94 package of programs²⁴ was used. Computations were carried out using three initial geometries (Figure 1): a D_{3h} tricapped trigonal prism, a C_{4v} capped square antiprism, and a C_{4v} capped cube. It is possible that a molecular dynamics simulation could identify other local minima, but such a thorough investigation of the potential surface was outside the scope of this paper.

The geometries were optimized without symmetry restrictions. Except as noted in Table 1, the vibrational analyses show that all of the optimized structures discussed in this paper are genuine minima at the B3LYP/LANL2DZdp level without any imaginary frequencies ($N_{\text{imag}} = 0$). The optimized structures found for the Ge_9^z clusters ($z = -6, -4, -3, -2, 0$, and $+2$) are summarized in Table 1 and depicted in Figures 2–7.

Since the highly negatively charged clusters are calculated at the present level to be unstable in the gas phase relative to the loss

- (21) Becke, A. D. *J. Chem. Phys.* **1993**, *98*, 5648.
- (22) Hay, P. J.; Wadt, W. R. *J. Chem. Phys.* **1985**, *82*, 270, 284, 299.
- (23) Check, C. L.; Faust, T. O.; Bailey, J. M.; Wright, B. J.; Gilbert, T. M.; Sunderlin, L. S. *J. Phys. Chem. A* **2001**, *105*, 8111.
- (24) Frisch, M. J.; Trucks, G. W.; Schlegel, H. B.; Gill, P. M. W.; Johnson, B. G.; Robb, M. A.; Cheeseman, J. R.; Keith, T.; Petersson, G. A.; Montgomery, J. A.; Raghavachari, K.; Al-Laham, M. A.; Zakrzewski, V. G.; Ortiz, J. V.; Foresman, J. B.; Cioslowski, J.; Stefanov, B. B.; Nanayakkara, A.; Challacombe, M.; Peng, C. Y.; Ayala, P. Y.; Chen, W.; Wong, M. W.; Andres, J. L.; Replogle, E. S.; Gomperts, R.; Martin, R. L.; Fox, D. J.; Binkley, J. S.; Defrees, D. J.; Baker, J.; Stewart, J. P.; Head-Gordon, M.; Gonzalez, C.; Pople, J. A. *Gaussian 94*, revision C.3; Gaussian, Inc.: Pittsburgh, PA, 1995.

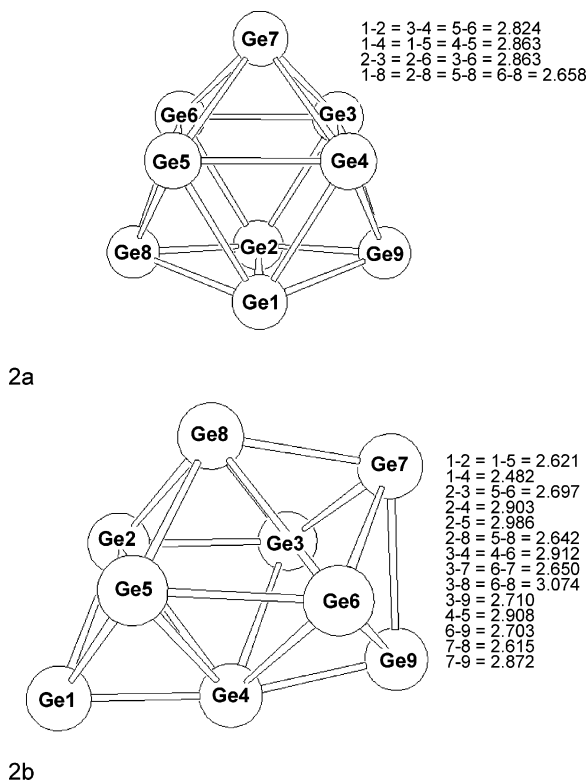


Figure 2. (a) Tricapped trigonal prism optimized structure for Ge_9^{2-} . (b) Capped bisdisphenoid optimized structure for Ge_9^{2-} , which is 15.58 kcal/mol above the tricapped trigonal prism.

of electrons, the effect of the positive counterions was simulated by adding suitable fractional positive charges q around the Ge_9^{2-} ($z = -2, -3, -4, -6$) clusters. These charges were distributed on the Connolly surfaces²⁵ generated using the Molekel package.²⁶ In each case, $q = z/N$ (N = number of points defining the Connolly surface) so that an Nq positive charge compensates for the negative charge of the cluster.

3. Results

3.1 20-Skeletal Electron Ge_9^{2-} . The cluster Ge_9^{2-} has 20 skeletal electrons corresponding to $2n + 2$ electrons for $n = 9$. Wade's rules^{5,6} thus predict the tricapped trigonal prism (Figure 1) for this structure. The lowest energy structure found computationally for Ge_9^{2-} by DFT optimizations starting from either the tricapped trigonal prism or the capped square antiprism is indeed the tricapped trigonal prism (Figure 2a). The same global minimum geometry was found also when the B3PW91 combination of Becke's three-parameter hybrid functional (HF exchange DFT exchange-correlation) with the Perdew–Wang 91 correlation functional was used in conjunction with the 6-311G(d) basis set for the optimizations.¹⁹

A second structure for Ge_9^{2-} of higher energy by 15.58 kcal/mol has been found by starting the optimization from the capped cube. This structure (Figure 2b) may be described as a Ge_8 bisdisphenoid with the ninth germanium atom capping one of the faces.

3.2 Electron-Rich Structures. There is a large amount of experimental information on Ge_9^{4-} structures with various counterions as well as E_9^{4-} anions of the other group 14 elements from silicon to lead.^{7,27,28} Both the capped square antiprismatic (C_{4v}) and tricapped trigonal prismatic (D_{3h}) geometries (Figure 1) are found. The capped square antiprismatic geometry with a single nontriangular face is predicted by Wade's rules for a nido compound with the $2n + 4$ skeletal electrons of Ge_9^{4-} . The tricapped trigonal prismatic rather than the capped square antiprismatic geometry is found experimentally in the isoelectronic Bi_9^{5+} cation.²⁹

Our computations for the Ge_9^{4-} cluster indicate that the capped square antiprismatic and tricapped trigonal prismatic structures (Figure 3a,b) have very similar energies. The minimum energy structure for Ge_9^{4-} is actually a tricapped trigonal prism, but the capped square antiprism is only 0.21 kcal/mol higher in energy with only a single very small imaginary frequency (12i). This is in accord with the fluxionality of the closely related Sn_9^{4-} and Pb_9^{4-} ions observed experimentally by metal NMR.^{8,9} Note that at the B3PW91 level the capped square antiprismatic structure is reported²⁰ to be a global minimum while the B3LYP/6-311+G** calculations of Hirsch et al.¹⁹ lead to the same ordering as reported here. For the analogous silicon cluster Si_9^{4-} , the C_{4v} capped square antiprismatic structure is calculated²⁸ to be 0.52 kcal/mol more stable than the D_{3h} tricapped trigonal prismatic structure at the HF/6-31G(D) level.

Optimization of the Ge_9^{4-} cluster from the capped cube led to neither the capped square antiprism nor the tricapped trigonal prism but instead to a third type of structure 24.27 kcal/mol above the lowest energy structure. This structure (Figure 3c) can be described as a capped bisdisphenoid closely related to the optimized structure for Ge_9^{2-} obtained from the capped cube.

The electron-rich "free radical" Ge_9^{3-} cluster is also known experimentally as a tricapped trigonal prism in the structures of the type $[\text{K}(\text{cryptand})^+]_3\text{Ge}_9^{3-} \cdot 2\text{L}$ ($\text{L} = \text{PPh}_3$ or $2\text{L} = \text{H}_2\text{NCH}_2\text{CH}_2\text{NH}_2$).^{30,31} The same optimized tricapped trigonal prismatic structure with a rigorous C_1 rather than the idealized D_{3h} symmetry (Figure 4a) is computed from any of the three starting points used in this work.

The final electron-rich germanium cluster stoichiometry studied in this work was Ge_9^{6-} with $24 = 2n + 6$ skeletal electrons. By Wade's rules^{5,6} this should be an arachno structure with a large open face similar to the structures of the two isomeric B_9H_{15} nonaboranes with a hexagonal or heptagonal^{32,33} open face.³⁴ However, the optimized structure

(25) Connolly, M. L. *J. Am. Chem. Soc.* **1985**, *107*, 1118.

(26) Portmann, S. *Molekel*, version 4.3.win32, Date 11.Nov.02; University of Geneva, Geneva, 2002; CSCS/ETH.

(27) Quéneau, V.; Todorov, E.; Sevov, S. C. *J. Am. Chem. Soc.* **1998**, *120*, 3263.

(28) von Schnering, H. G.; Somer, M.; Kaupp, M.; Carillo-Cabrera, W.; Basitinger, M.; Schmeding, A.; Grin, Y. *Angew. Chem., Int. Ed.* **1998**, *37*, 2359.

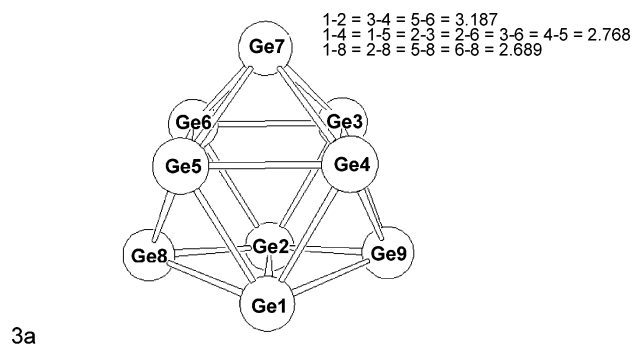
(29) Friedman, R. M.; Corbett, J. D. *Inorg. Chem.* **1973**, *12*, 1134.

(30) Belin, C.; Mercier, H.; Angilella, V. *New J. Chem.* **1991**, *15*, 931.

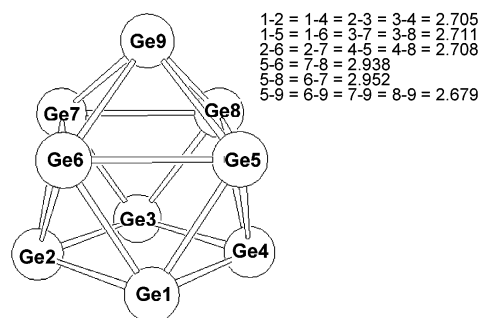
(31) Fässler, T.; Hunziker, *Inorg. Chem.* **1994**, *33*, 5380.

(32) Dickerson, R. E.; Wheatly, P. H.; Howell, P. A.; Lipscomb, W. N. *J. Chem. Phys.* **1957**, *27*, 200.

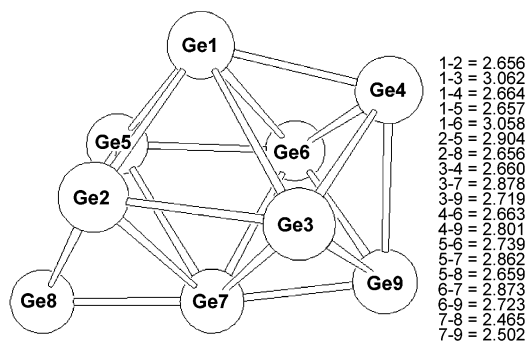
(33) Simpson, P. G.; Lipscomb, W. N. *J. Chem. Phys.* **1961**, *35*, 1340.



3a



3b



3c

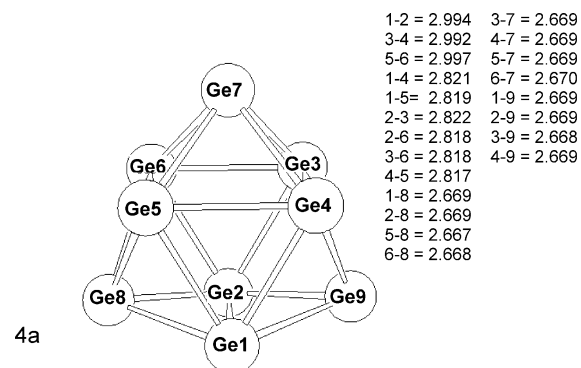
Figure 3. (a) Tricapped trigonal prism optimized structure for Ge_9^{4-} . (b) Capped square antiprism optimized structure for Ge_9^{4-} , which is only 0.21 kcal/mol above the tricapped trigonal prism. (c) Capped bisdisphenoid optimized structure for Ge_9^{4-} , which is 15.58 kcal/mol above the tricapped trigonal prism.

computed for Ge_9^{6-} is a highly distorted tricapped trigonal prism with one unusually long (3.11 Å) horizontal edge (edge 7–8 in Figure 4b). This suggests some type of Jahn–Teller distortion. Recomputing the Ge_9^{6-} stoichiometry as a triplet rather than a singlet led also to a tricapped trigonal prism but with very little distortion (0.01 Å) from ideal D_{3h} symmetry (Figure 4c). The triplet Ge_9^{6-} optimized structure was found to be slightly lower in energy (3.66 kcal/mol) than the singlet.

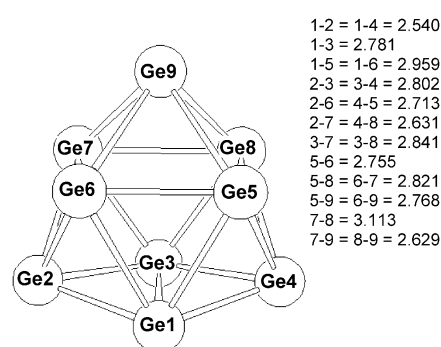
3.3 Electron-Poor Structures. The $18 = 2n$ skeletal electron cluster is neutral Ge_9 , which has been observed in the gas phase.³⁵ However, neutral Ge_9 probably cannot be isolated in the solid state because of polymerization to elemental germanium. Nevertheless, the isoelectronic Tl_9^{9-} has been found in the intermetallics $\text{Na}_2\text{K}_{21}\text{Tl}_{19}$ (ref 36) and

(34) Bould, J.; Greatrex, R.; Kennedy, J. D.; Ormsby, D. L.; Londesborough, M. G. S.; Callaghan, K. L. F.; Thornton-Pett, M.; Spalding, T. R.; Teat, S. J.; Clegg, W.; Fang, H.; Rath, N. P.; Barton, L. *J. Am. Chem. Soc.* **2002**, *124*, 7429.

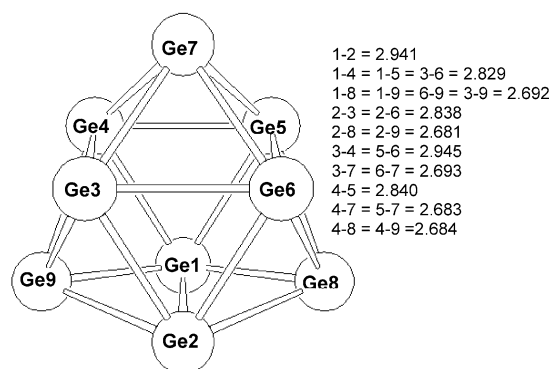
(35) Zhao, J. J.; Wang, J. L.; Wang, G. H. *Phys. Lett. A* **2000**, *275*, 281.



4a



4b



4c

Figure 4. (a) Tricapped trigonal prism optimized structure for Ge_9^{3-} . (b) Distorted tricapped trigonal prism optimized structure for singlet Ge_9^{6-} . (c) Tricapped trigonal prism optimized structure for triplet Ge_9^{6-} .

$\text{Na}_{12}\text{K}_{38}\text{Tl}_{48}\text{Au}_2$ (ref 37). The structure of Tl_9^{9-} is shown by X-ray crystallography to be a nine-vertex C_{2v} deltahedron conveniently described as a monoflattened tricapped trigonal prism,^{38,39} namely a tricapped trigonal prism with one of the caps pushed in toward the center of the polyhedron. A very closely related neutral Ge_9 structure (Figure 5a) is computed starting from either a tricapped trigonal prism or a capped square antiprism. However, a bicapped pentagonal pyramid structure (Figure 5b) of 4.54 kcal/mol lower energy is found for Ge_9 starting from the capped cube. This appears to be the global minimum since it has been reached by using several other methods^{12,13,16} including ab initio molecular dynamics studies.^{14,15}

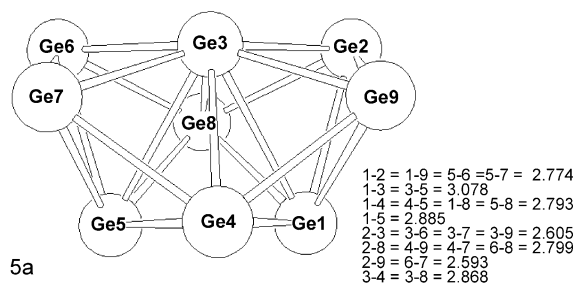
The optimized structures for the dication Ge_9^{2+} ($a(16 = 2n - 2)$ -skeletal electron stoichiometry) can be described by

(36) Dong, Z.-C.; Corbett, J. D. *J. Am. Chem. Soc.* **1994**, *116*, 3429.

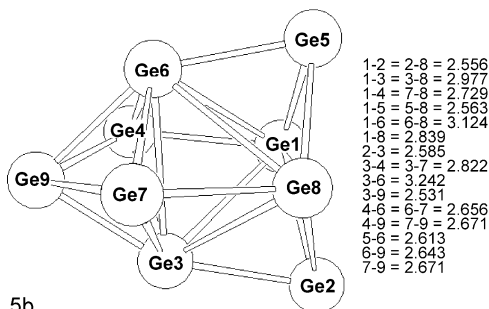
(37) Henning, R. W.; Corbett, J. D. *Inorg. Chem.* **1997**, *36*, 6045.

(38) King, R. B. *Inorg. Chim. Acta* **1996**, *252*, 115.

(39) King, R. B. *Inorg. Chem.* **2002**, *41*, 4722.

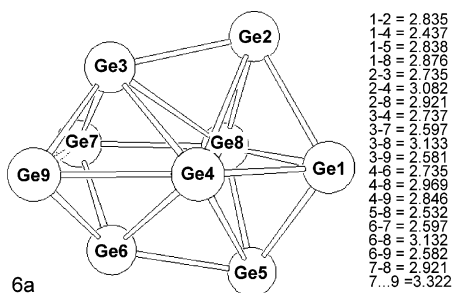


5a

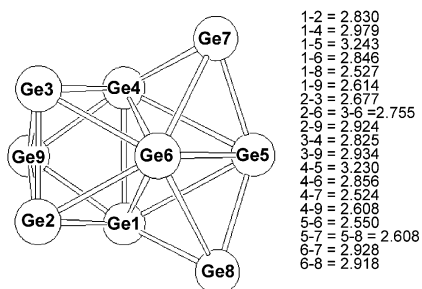


5b

Figure 5. (a) Flattened tricapped trigonal prism optimized structure for Ge_9 similar to the experimentally found structure for the isoelectronic Tl_9^{9-} . (b) Bicapped pentagonal bipyramid global minimum for Ge_9 .



6a

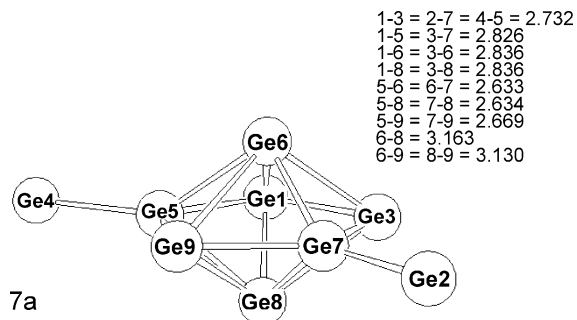


6b

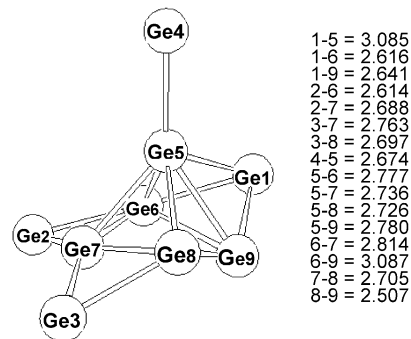
Figure 6. (a) Global minimum found for Ge_9^{2+} consisting of the fusion of an octahedron and two trigonal bipyramids. (b) A slightly higher energy structure (5.38 kcal/mol) found for Ge_9^{2+} .

the fusion of three deltahedra. The lowest energy optimized structure for Ge_9^{2+} found by starting with either the capped cube or the capped square antiprism can be described as a fusion of an octahedron with two trigonal bipyramids (Figure 6a). A slightly higher energy structure for Ge_9^{2+} by 3.6 kcal/mol can be described as a fusion of an octahedron with two tetrahedra (Figure 6b). Related structures consisting of three fused deltahedra are found in iridium carbonyl clusters⁴⁰ such as $\text{Ir}_{10}(\text{CO})_{21}^{2-}$ (two octahedra plus a trigonal bipyramid)⁴¹ and $\text{Ir}_{11}(\text{CO})_{23}^{3-}$ (three octahedra).⁴²

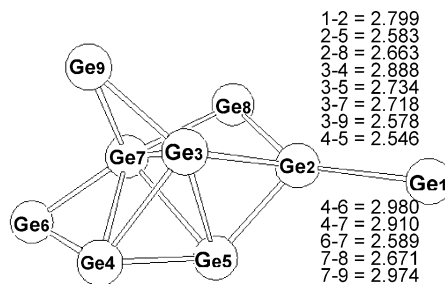
The lowest energy optimized structure for the tetracation Ge_9^{4+} was found to be an oblate (squashed) pentagonal bi-



7a



7b



7c

Figure 7. (a) Global minimum for Ge_9^{4+} with two pendant Ge atoms on a central Ge_7 oblate pentagonal bipyramid. (b and c) Two higher energy open structures found for Ge_9^{4+} .

pyramid with two external pendant Ge vertices (Figure 7a). This structure was obtained by starting from the capped square antiprism. The oblate pentagonal bipyramidal geometry may relate to the 14 skeletal electrons in Ge_9^{4+} . Previous work³ showed that the lowest energy computed structure for Ge_7 with 14 skeletal electrons was also an oblate pentagonal bipyramid. This could imply that the two pendant Ge vertices on the oblate pentagonal bipyramid in the lowest energy Ge_9^{4+} structure are net donors of zero skeletal electrons, which would be the case if their four valence electrons were two external lone pairs. Starting with the C_{4v} capped cube or D_{3h} tricapped trigonal prism led to optimized structures for Ge_9^{4+} of higher energies with very open geometries and no obvious symmetry (Figure 7b,c).

4. Discussion

4.1 Energies. Figure 8 plots the computed energies for the lowest energy structures of the Ge_9^z clusters ($z = -6, -4, -3, -2, 0,$ and $+2$) against their charges using the

(40) King, R. B. *Inorg. Chim. Acta* **2002**, *334*, 34.

(41) Della Pergola, R.; Cea F.; Garlaschelli, L.; Masciocchi, N.; Sansoni, M. *J. Chem. Soc., Dalton Trans.* **1994**, 1501.

(42) Della Pergola, R.; Garlaschelli, L.; Sansoni, M. *J. Cluster Sci.* **1999**, *10*, 109.

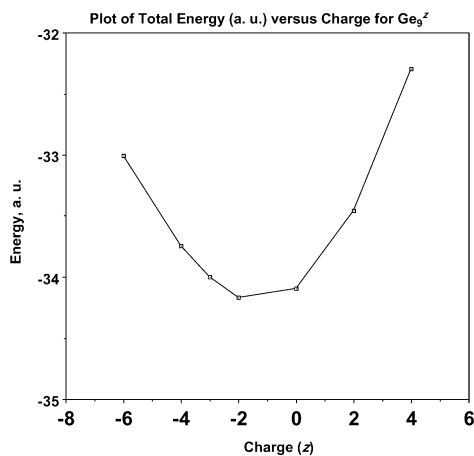


Figure 8. Plot of total energy (atomic units) as a function of charge for the Ge₉^z clusters.

singlet structure for Ge₉⁶⁻. This plot reflects the instability of the isolated highly charged clusters, either positive or negative. By taking into account (even in a very approximate manner) the presence of the positive counterions (Table 1), the highly negative clusters are stabilized.

The four lowest energy structures are Ge₉²⁻ < Ge₉ < Ge₉³⁻ < Ge₉⁴⁻. All of these species or close isoelectronic analogues (e.g., Tl₉⁹⁻ ≈ Ge₉) have been realized experimentally with structures very similar to the computed structures as already discussed. The more highly charged species (Ge₉⁶⁻ and Ge₉⁴⁺) with higher energies have not yet been realized experimentally.

4.2 Molecular Orbitals of the Tricapped Trigonal Prismatic and Capped Square Antiprismatic Clusters.

Our previous papers on the five-, six-, and seven-vertex bipyramidal clusters¹⁻³ have depicted their bonding molecular orbitals (MOs) using the terminology of tensor surface harmonic theory.⁴³⁻⁴⁷ Figures 9 and 10 compare the shapes of the 20 lowest lying bonding MOs computed for the tricapped trigonal prismatic Ge₉²⁻ cluster (Figure 2a) and the capped square antiprismatic Ge₉⁴⁻ cluster (Figure 3a). The energies of these MOs are listed in Table 2. The irreducible representations (irreps) for the MOs of the external lone pairs (Γ_σ) and the surface bonding (Γ_π) are listed in Table 3 for both of the polyhedra of interest. The external lone pair MOs belong to the same irreps as the nine atomic orbitals of the sp³d⁵ atomic orbital manifold in nine-coordinate tricapped trigonal prismatic and capped square antiprismatic complexes since both of these polyhedra for nine-coordination can be formed from the sp³d⁵ nine-orbital manifold without using f orbitals. The single bonding MO for the multicenter core bond in Ge₉²⁻ belongs to the fully symmetrical irrep and is thus an S orbital without any nodes. The core and external bonding orbitals of S symmetry can mix either in phase or out of phase to give S⁺ and S⁻ bonding MOs, respectively. Thus, the 10 lowest lying bonding MOs

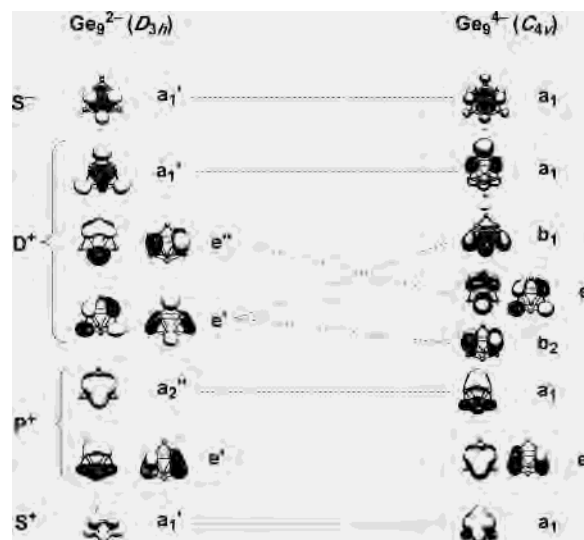


Figure 9. Comparison of the 10 lowest lying bonding MOs for tricapped trigonal prismatic Ge₉²⁻ and capped square antiprismatic Ge₉⁴⁻.

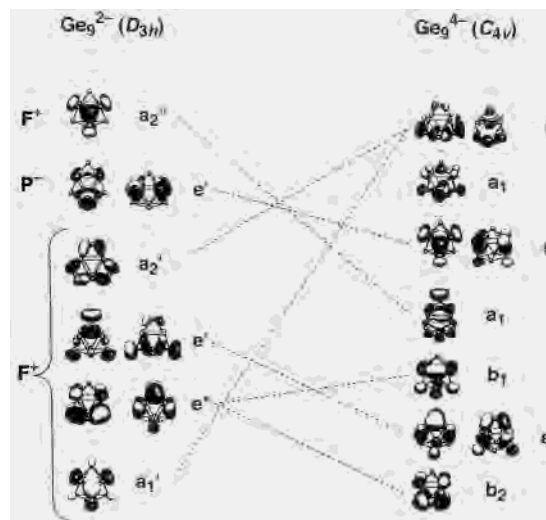


Figure 10. Comparison of the remaining bonding MOs for for tricapped trigonal prismatic Ge₉²⁻ and capped square antiprismatic Ge₉⁴⁻.

in both the tricapped trigonal prismatic and capped square antiprismatic clusters correspond to the two S[±] orbitals, the three P⁺ orbitals, and the five D⁺ orbitals and have the shapes and nodal patterns of the corresponding atomic orbitals (Figure 9). These 10 bonding MOs may be considered to correspond approximately to the multicenter core bond and the external lone pairs.

The remaining bonding MOs for both Ge₉²⁻ and Ge₉⁴⁻ are depicted in Figure 10. These orbitals correspond to the seven F⁺ orbitals and two or three P⁻ orbitals and again have shapes and nodal patterns generally recognizable as similar to the corresponding atomic orbitals. These orbitals arise mainly from surface bonding and are seen to have the ungerade symmetry of P or F orbitals in accord with their formation through overlap of ungerade tangential p atomic orbitals on the vertex atoms.

4.3 Geometrical Relationships. The tricapped trigonal prism and capped square antiprism are closely related by a single diamond-square process (Figure 1a) involving rupture

(43) Stone, A. J. *Mol. Phys.* **1980**, *41*, 1339.

(44) Stone, A. J. *Inorg. Chem.* **1981**, *20*, 563.

(45) Stone, A. J.; Alderton, J. J. *Inorg. Chem.* **1982**, *21*, 2297.

(46) Stone, A. J. *Polyhedron* **1984**, *3*, 1299.

(47) Johnston, R. L.; Mingos, D. M. P. *Theor. Chim. Acta* **1989**, *75*, 11.

Table 2. Molecular Orbital Energies and Symmetry/Tensor Surface Harmonic Labels for Tricapped Trigonal Prismatic Ge_9^{2-} and Ge_9^{4-} (D_{3h}) and Capped Square Antiprismatic Ge_9^{4-} ($\sim C_{4v}$)^{a,b}

	Ge_9^{2-} (D_{3h})	Ge_9^{4-} (D_{3h})	Ge_9^{4-} ($\sim C_{4v}$)
1	-0.35645/-0.54173 (a_1') S^+	-0.14752/-0.48363(a_1') S^+	-0.14534/-0.48330 (a_1) S^+
2	-0.27381/-0.45915 (e') P^+	-0.06137/-0.39793(a_2'') P^+	-0.05904/-0.39729 (e) P^+
3	-0.27381/-0.45913 (e') P^+	-0.05778/-0.39491(e') P^+	-0.05860/-0.39728 (e) P^+
4	-0.23587/-0.42131 (a_2'') P^+	-0.05778/-0.39486(e') P^+	-0.05312/-0.39204 (a_1) P^+
5	-0.14686/-0.33225 (e') D^+	0.05564/-0.28220(e'') D^+	0.05636/-0.28334 (b_2) D^+
6	-0.14686/-0.33224 (e') D^+	0.05564/-0.28213(e'') D^+	0.06285/-0.27701 (e) D^+
7	-0.13099/-0.31655 (e'') D^+	0.07128/-0.26721(e') D^+	0.06346/-0.27655 (e) D^+
8	-0.13099/-0.31653 (e'') D^+	0.07128/-0.26718(e') D^+	0.07996/-0.25926(b_1) D^+
9	-0.11018/-0.29562 (a_1') D^+	0.07998/-0.25818(a_1') D^+	0.08087/-0.25954(a_1) D^+
10	-0.00963/-0.19540 (a_1') S^-	0.18625/-0.15364(a_1') S^-	0.18819/-0.15342 (a_1) S^-
11	0.02542/-0.16012 (a_1') F^+	0.21847/-0.12079(e'') F^+	0.21698/-0.12371 (b_2) F^+
12	0.02647/-0.15912 (e'') F^+	0.21847/-0.12073(e'') F^+	0.22803/-0.11316 (e) F^+
13	0.02647/-0.15909 (e'') F^+	0.23391/-0.10579(e') F^+	0.22854/-0.11252 (e) F^+
14	0.02980/-0.15555 (e') F^+	0.23391/-0.10575(e') F^+	0.23543/-0.10599 (b_1) F^+
15	0.02980/-0.15551 (e') F^+	0.23668/-0.10335(a_1') F^+	0.23798/-0.10391 (a_1) F^+
16	0.03240/-0.15305 (a_2') F^+	0.24327/-0.09677(a_2'') F^+	0.24718/-0.09437 (e) P^-
17	0.05577/-0.12991 (e') P^-	0.25108/-0.08910(e') P^-	0.24760/-0.09410 (e) P^-
18	0.05577/-0.12988 (e') P^-	0.25108/-0.08906(e') P^-	0.25513/-0.08628 (a_1) P^-
19	0.06262/-0.12290 (a_2'') F^+	0.25119/-0.08878(a_2') F^+	0.26716/-0.07429 (e) F^+
20	0.13763/-0.04732 (a_2'') P^-	0.27644/-0.06260(a_2'') P^-	0.26787/-0.07277 (e) F^+

^a The values for the HOMO are italicized in each column. MOs below the italicized entries are unoccupied MOs starting with the LUMO. ^b The second value in each cell corresponds to the orbital energy of the system surrounded by the appropriate positive charges distributed on the Connolly surface.

Table 3. Irreducible Representations for the Molecular Orbitals in Nine-Vertex Polyhedra

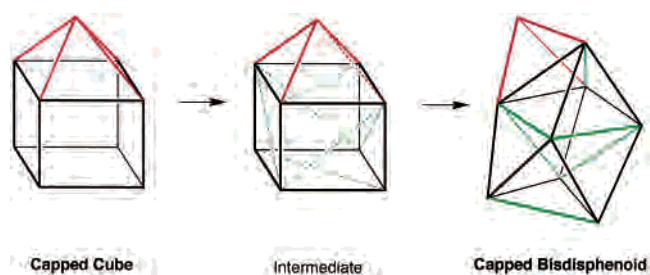
Tricapped Trigonal Prism	
Γ_σ	$2A_1'(s; z^2) + 2E'(x, y; x^2-y^2, xy) + A_2''(z) + E''(xz, yz)$
Γ_π	$A_1' + 2A_2' + 3E' + A_1'' + 2A_2'' + 3E''$
Capped Square Antiprism	
Γ_σ	$3A_1(s; z; z^2) + B_1(x^2-y^2) + B_2(xy) + 2E(x, y; xz, yz)$
Γ_π	$2A_1 + 2A_2 + 2B_1 + 2B_2 + 5E$

Table 4. Dimensions of Some Tricapped Trigonal Prismatic Clusters

cluster	v/h ratio	lit. ref
20 Skeletal Electron Clusters		
Ge_9^{2-}	0.99	this work
Ge_9^{2-}	1.03	50
$\text{B}_9\text{Br}_9^{2-}$	0.89	51
$\text{B}_9\text{H}_9^{2-}$	0.97	10
$\text{B}_7\text{H}_7\text{C}_2\text{Me}_2$	0.90	10
21 Skeletal Electron Cluster		
Ge_9^{3-}	1.06	this work
Ge_9^{3-}	1.17	31
22 Skeletal Electron Clusters		
Ge_9^{4-}	1.15	this work
Bi_9^{5+}	1.15	29
24 Skeletal Electron Cluster		
Ge_9^{6-} (triplet)	1.04	this work

of an edge connecting two degree 5 vertices of the tricapped trigonal prism. It is thus not surprising that they are readily interconverted in fluxional processes or that a capped square antiprism is easily reached in the DFT optimization process for Ge_9^{4-} starting with a tricapped trigonal prism. This relationship between the tricapped trigonal prism and the capped square antiprism is well documented in the literature.

In 1976, Guggenberger and Muetterties¹⁰ first described the shapes of tricapped trigonal prismatic molecules by the ratio of the length of the prism “height” (i.e., vertical distance, v) to the basal edge length (i.e., horizontal distance, h) depicted in Figure 1a. Subsequently, one of us⁴⁸ noted the relationship of the skeletal electron count of a tricapped

**Figure 11.** Relationship between the capped cube and the capped bisdisphenoid color coding the edges as follows: black, edges arising from the 12 edges of the original cube; red, edges from the cap; green, edges arising from the six diagonals added to the original cube.

trigonal prism cluster to this v/h ratio (Table 4). Thus, the v/h ratio was found to fall in the range 0.9–1.0 for 20-skeletal electron clusters such as $\text{B}_9\text{H}_9^{2-}$ (ref 49), $\text{B}_7\text{H}_7\text{C}_2\text{Me}_2$ (ref 49), and Ge_9^{2-} (ref 50) but 1.15 for the 22-skeletal electron cluster Bi_9^{5+} (ref 29). In the current work, we compute a v/h ratio of 1.15 for Ge_9^{4-} with tricapped trigonal prismatic geometry. The v/h ratios computed for the tricapped trigonal prisms in Ge_9^{3-} and Ge_9^{6-} (triplet) are both very similar despite their different skeletal electron counts, namely 1.05 ± 0.01 .

A more unusual observation from this work is the accessibility of a new type of nine-vertex deltahedron from the capped cube by the DFT optimization process in both the Ge_9^{4-} and Ge_9^{2-} systems (Figure 11). This new deltahedron can be derived from the most spherical eight-vertex deltahedron,⁴ namely the bisdisphenoid, by capping a triangular face with two vertices of initial degree 4 and a third vertex of initial degree 5. This leads to a deltahedron

(49) Guggenberger, L. J.; Muetterties, E. L. *J. Am. Chem. Soc.* **1976**, *98*, 7221.

(50) Belin, C. H. E.; Corbett, J. D.; Cisar, A. *J. Am. Chem. Soc.* **1977**, *99*, 7163.

(51) Hönle, W.; Grin, Y.; Burckhardt, A.; Wedig, U.; Schultheiss, M.; von Schnering, H. G.; Kallner, R.; Binder, H. *J. Solid State Chem.* **1997**, *133*, 59.

(48) King, R. B. *Inorg. Chim. Acta* **1982**, *57*, 79.

with one vertex of degree 3, two vertices of degree 4, five vertices of degree 5, and one vertex of degree 6.

Figure 11 shows the relationship between the capped cube and the capped bisdisphenoid. In the capped cube, the edges of the underlying cube are depicted in black, and the additional four edges to the cap are depicted in red. Conversion of a cube to a bisdisphenoid involves adding six diagonals (green lines in Figure 11) followed by distortions so that the lengths of the diagonals and the edges of the original cube are very similar. In the case of the conversion of the capped cube to the capped bisdisphenoid depicted in Figure 11, one of the four edges to the cap (the red dashed line) is broken as the cube distorts to a bisdisphenoid. In the final capped bisdisphenoid depicted in Figure 11, the 12 edges of the original cube are depicted in black, the three edges remaining to the cap are depicted in red, and the six edges from the diagonal are depicted in green.

5. Summary

The computations described in this paper give results consistent with experimental data on nine-vertex germanium clusters and isoelectronic species. Thus, the computed global minimum for the germanium cluster Ge_9^{2-} is a tricapped

trigonal prism in accord with Wade's rules for a $2n + 2$ skeletal electron structure.^{5,6} A somewhat elongated tricapped trigonal prism is the global minimum for Ge_9^{4-} similar to the experimentally found structure for the isoelectronic Bi_9^{5+} . However, the capped square antiprism predicted by Wade's rules for a $2n + 4$ skeletal electron structure is only 0.21 kcal/mol above this global minimum indicating that these two structures have very similar energies. The global minimum for the neutral cluster Ge_9 was found to be a bicapped pentagonal bipyramid. However, a second structure for Ge_9 only 4.54 kcal/mol above this global minimum is the C_{2v} flattened tricapped trigonal prism found experimentally for the isoelectronic Tl_9^{9-} .

Acknowledgment. We are indebted to the National Science Foundation for partial support of this work under Grant CHE-0209857. Part of this work was undertaken with the financial support from CNCSIS-Roumania through Grant 23/2002. We are also indebted to Prof. H. F. Schaefer, III, of the University of Georgia Center for Computational Quantum Chemistry for providing computational facilities used in this work.

IC030107Y